Available online at www.sciencedirect.com
ScienceDirect
Journal of the European Ceramic Society 26 (2006) 3647–3656
www.elsevier.com/locate/jeurceramsoc

Modelling the mechanical properties of microporous and macroporous biphasic calcium phosphate bioceramics

F. Tancret [a,*], J.-M. Bouler [b], J. Chamousset [a,c], L.-M. Minois [a]

[a] *Laboratoire Génie des Matériaux et Procédés Associés, Polytech'Nantes, La Chantrerie, rue Christian Pauc, BP 50609, 44306 Nantes cedex 3, France*
[b] *INSERM EM99-03, "Matériaux d'Intérêt Biologique", Faculté de Chirurgie Dentaire, 1, place Alexis Ricordeau, BP 84215, 44042 Nantes cedex 1, France*
[c] *BIOMATLANTE, ZA des quatre Nations, 44360 Vigneux de Bretagne, France*

Received 29 September 2005; received in revised form 9 December 2005; accepted 16 December 2005
Available online 21 February 2006

Abstract

Macroporous biphasic calcium phosphate bioceramics, for use as bone substitutes, have been fabricated by cold isostatic pressing and conventional sintering, using naphtalen particles as a porogen to produce macropores. The resulting ceramics, composite materials made of hydroxyapatite and β-tricalcium phosphate (TCP) containing ∼45% macropores and with various microporosities, have been submitted to compression and three-point bending tests, toughness tests by single-edge-notched-bending (SENB), and spherical indentation tests. By combining two approaches at two different scales, one for closed porosity and one for open porosity, a model is established to describe mechanical properties as a function of the amount and morphology of porosity. The model assumes a quasi-continuous matrix containing macropores, the matrix being itself microporous, and considers that fracture always initiates on a macropore. The preliminary mechanical tests performed on the sintered ceramics tend to validate the modelling approach.

Keywords: Fracture; Apatite; Porosity; Mechanical properties; Modelling

1. Introduction

Calcium phosphate bone substitutes have been used for many years.[1–3] Among them, the mostly used ones are hydroxyapatite (HA), $Ca_{10}(PO_4)_6(OH)_2$, which structure is close to that of biological apatites, β-tricalcium phosphate (TCP), $Ca_3(PO_4)_2$,[4–6] and biphasic calcium phosphates (BCP) made of a mixture of HA and TCP. They have the advantage to combine the physico-chemical properties of both compounds: the dissolution of TCP allows to obtain a local calcium and phosphate ion supersaturation, and the nucleation properties of HA favour the precipitation of biological apatites.[7] By adapting the proportions of HA and TCP, it is possible to control both resorption of BCP and osteoconduction.[8] BCP have been widely used for many years in human surgery as bone substitute materials.[9] Indeed, their chemical composition, close to those of mineral bone phases, provides them with adapted biological properties to serve as bone substitution materials.[8,10–12] BCP are therefore widely used for various clinical applications such as periodontal bone defects,[13] various orthopaedic applications,[5] as well as face and jaw surgery.[14]

To obtain an efficient bone substitute that can be degraded by bone cells and therefore be replaced by bone, there is a need for an adapted porous structure.[12] BCP sintered using a porogen to create macropores are currently the prime candidates as resorbable bone substitutes. A double scale porous microstructure is thus obtained, made of micropores in the sintered ceramic and of macropores created in the latter by the porogen. Micropores, resulting from the incomplete sintering of the pressed powder, are of the order of a micrometer; the macropores left by the porogen are of the order of several hundreds of micrometer.[15] When into contact with bone, these bioceramics stimulate bone ingrowth; the new cells grow within the material and progressively degrade it. In the end, in a matter of a several weeks, the ceramic is completely replaced by natural bone.

However, from a mechanical point of view, both HA and TCP present low mechanical properties in comparison with bone.[15] Consequently, one of the main drawbacks of macroporous BCP

* Corresponding author. Tel.: +33 2 40 68 31 97; fax: +33 2 40 68 31 99.
E-mail address: franck.tancret@univ-nantes.fr (F. Tancret).

0955-2219/$ – see front matter © 2006 Elsevier Ltd. All rights reserved.
doi:10.1016/j.jeurceramsoc.2005.12.015

ceramics is their brittleness and their low mechanical strength, which limits their use in case of important stresses. Therefore, it is necessary to optimise the mechanical properties of calcium phosphate bone substitutes. Nevertheless, this must not be achieved by degrading their osteoconduction properties, which is linked to macropores.[12] A compromise must thus be found between porosities and mechanical properties. It is therefore necessary to develop ceramics combining an excellent biocompatibility, a good resorption ability and high mechanical properties. To achieve simultaneously all these goals, these materials will have to contain a balanced amount of macropores—to allow the natural bone cells to grow inside the ceramic—and of interconnected micropores—to allow the impregnation of the material by biological fluids—the overall porosity being kept as low as possible to maintain good mechanical properties.[15]

However, it is well known that mechanical properties of materials depend on porosity.[16–24] With the levels of porosity encountered in macroporous bioceramics (sometimes higher than 75%), very low mechanical properties can be expected. To optimise the overall behaviour of such materials, it is therefore necessary to understand how microstructural parameters influence mechanical properties. In this aim, it would be useful to model the mechanical behaviour as a function of the amount and morphology of porosity. Nevertheless, no attempt has been made so far to model the influence of both microporosity and macroporosity on the mechanical properties of such materials, and only polynomial fits have been assessed.[25] In the present work, it is thus proposed to model the variation with porosity of mechanical properties—fracture strength, toughness and hardness—of some highly porous BCP bioceramics, taking into account the fact that both macropores and micropores of different morphologies coexist. Then, the models will be compared to preliminary measurements, such as to bring both a first assessment of the modelling approach and an understanding of the observed trends.

2. Materials and testing

2.1. Fabrication of materials

Some materials have been fabricated with various microstructures, in an attempt to perform a preliminary validation of the modelling approach proposed further. For this, calcium deficient apatite (CDA), of general formulation $Ca_{10-x}(HPO_4)_x(PO_4)_{6-x}(OH)_{2-x}$ $(0<x<2)$, is synthesized through the hydrolysis of $HCaPO_4, 2H_2O$ in an aqueous solution of NaOH, by heating for 4 h at 100 °C.[26] The chosen stoichiometry corresponds to a ratio Ca/P of 1.6 ($x=0.4$). The solution is then filtered, dried 48 h at 40 °C, and the remaining water is eliminated by a heat treatment of 1 h at 400 °C. The porogen, naphtalen particles of ~400 μm in diameter with a narrow distribution in size, is then mixed with the CDA powder in a Turbula® shaker-mixer. The amount of porogen corresponds to a final volume fraction of ~0.45. The resulting mix is then cold isostatically pressed under 140 MPa to the shape of bars. After elimination of the porogen at ~80 °C, and a plateau of 1 h at 400 °C to eliminate all residual traces of porogen and/or humidity, the ceramics are pressureless sintered under air for 3 to 8 h at temperatures between 950 and 1100 °C.

2.2. Structure and microstructure

Crystal structure is investigated by X-ray diffraction using the Cu Kα radiation. For ceramographic observation by optical microscopy and scanning electron microscopy (SEM), samples are cut from the sintered bars, impregnated in an epoxy resin under vacuum, and polished with SiC papers down to P1200 grade and then with diamond suspensions down to 3 μm in grain size. Macroporosity is then measured by quantitative image analysis on polished cross-sections.[27] Total porosity is estimated through the apparent density of specimens; the microporous volume is then obtained by subtracting the macroporous volume and the solid volume from the total volume.

2.3. Mechanical properties testing

Parallelepipedic bars of 10 mm × 10 mm × 50 mm are cut from the sintered blocks, and tested in three-point bending with a span of 40 mm, either to measure the flexural strength, or the fracture toughness in the single-edge-notched-bending (SENB) configuration. For the latter, a straight and sharp notch is introduced into the beams with a thin saw, with a depth, a, of about 40% of the beam height, w. This standard procedure has been validated on a wide range of brittle materials.[23,28] Compression testing is performed on parallelepipedic bars of 10 mm × 10 mm × 25 mm, the compressive force being applied on the largest sides. Hardness is finally measured through indentation tests using a 7 mm diameter steel bead under loads ranging from 100 to 400 N.

3. Experimental results and discussion

3.1. Structure and microstructure

During sintering, the CDA is transformed into a mixture of ~60% HA and ~40% TCP, as confirmed by X-ray diffraction on sintered ceramics.[29,30] As expected, when sintering time and temperature increase, total porosity decreases (Fig. 1). A typical SEM micrograph of a polished cross-section is shown in Fig. 2a. Quantitative image analysis yields a macropore volume fraction from 0.44 to 0.485 with respect to the total volume, depending on specimens.

3.2. Mechanical properties and fractographic observations

As can be seen on the SEM fractographs of Fig. 2b and c, rupture follows paths crossing macropores, by the fracture of thin walls between pores. At the micropore and grain scale, fracture proceeds by an intergranular mechanism, resulting from the fracture of individual sintering necks (Fig. 2d).

In all cases, as can be seen on Fig. 3, the measured mechanical properties are very low and subject to a high statistical dispersion, sometimes of the order of magnitude of the measurements

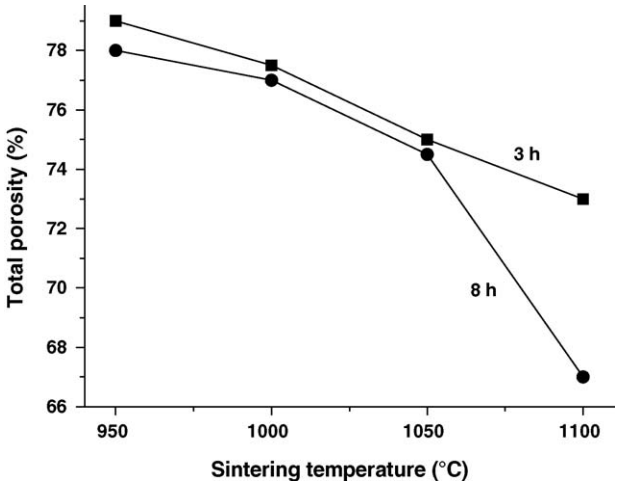

Fig. 1. Evolution of total porosity, p, as a function of sintering temperature and time.

themselves. It seems therefore difficult to extract precise evolutions of properties as a function of porosity, although globally decreasing trends can be identified. It is important to note at this point that error bars on Fig. 3 represent the statistical dispersion of measurements and not a conventional measurement uncertainty; this is why some points do not have an error bar (single measurement).

In these conditions of high statistical dispersion, it is clear that any theoretical model may not be precisely adjusted, nor its very principle even completely validated. Nevertheless, such a model may help to better understand and explain the measurements and, in fine, contribute to the optimisation or to the improvement of the materials properties for their applications. In this aim, a new model is developed in the next section to describe the evolution of mechanical properties of these bioceramics as a function of the amount and morphology of porosity.

4. Mechanical properties modelling

4.1. Theoretical background

In the past, much work has been done to model the variation with porosity of Young's modulus[16,17,19,20,31] and fracture properties[18,21–24,32] of materials. These models describing mechanical properties of materials as a function of porosity generally belong to one of the following two categories: some models refer to materials containing closed pores—for instance spherical pores—inside a continuous matrix, others describe the microstructure as the result of the densification of a stacking of

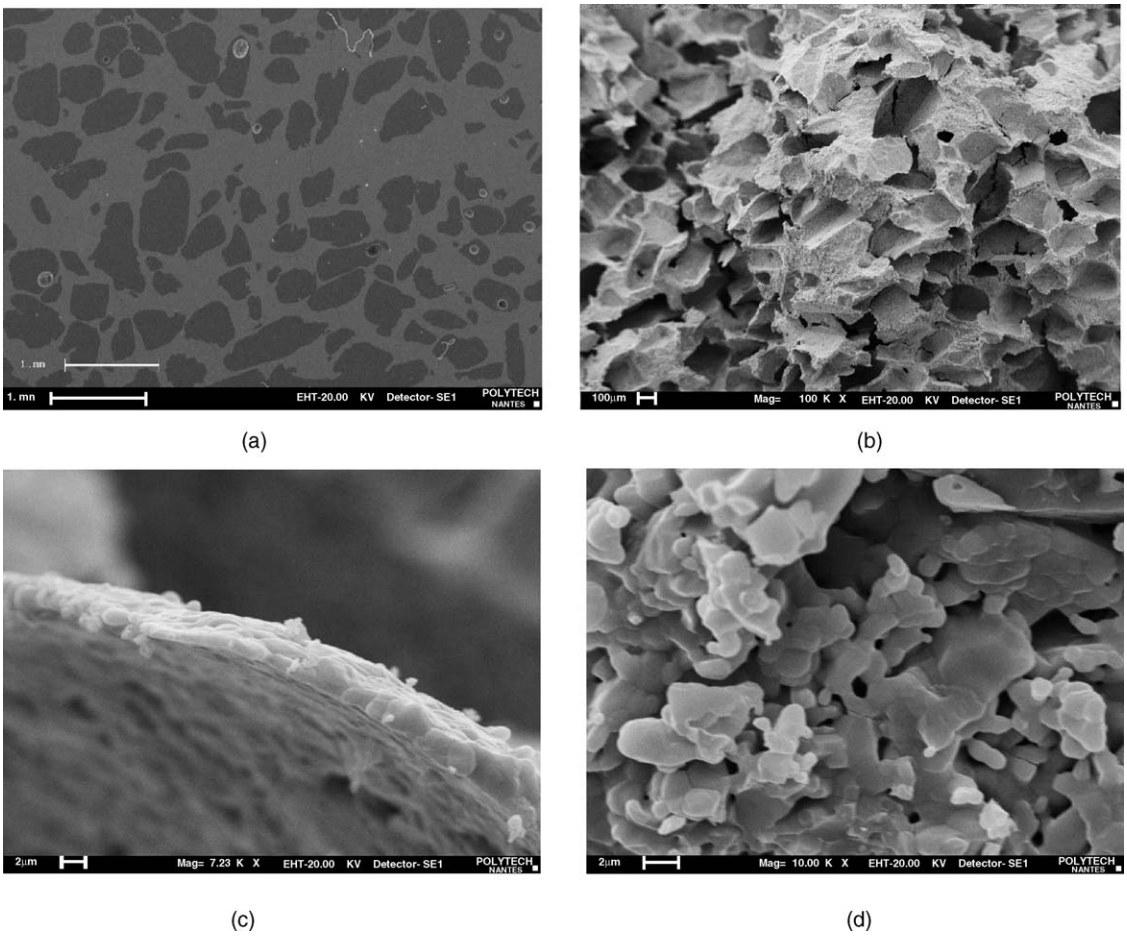

Fig. 2. (a) SEM image of a polished cross-section. Macropores are impregnated by an epoxy resin and appear dark. (b) Fractograph: at the macropore scale, the crack passes through the macropores. (c) Cracking proceeds by fracture of the thin walls between macropores. (d) Intergranular fracture at the micropore scale.

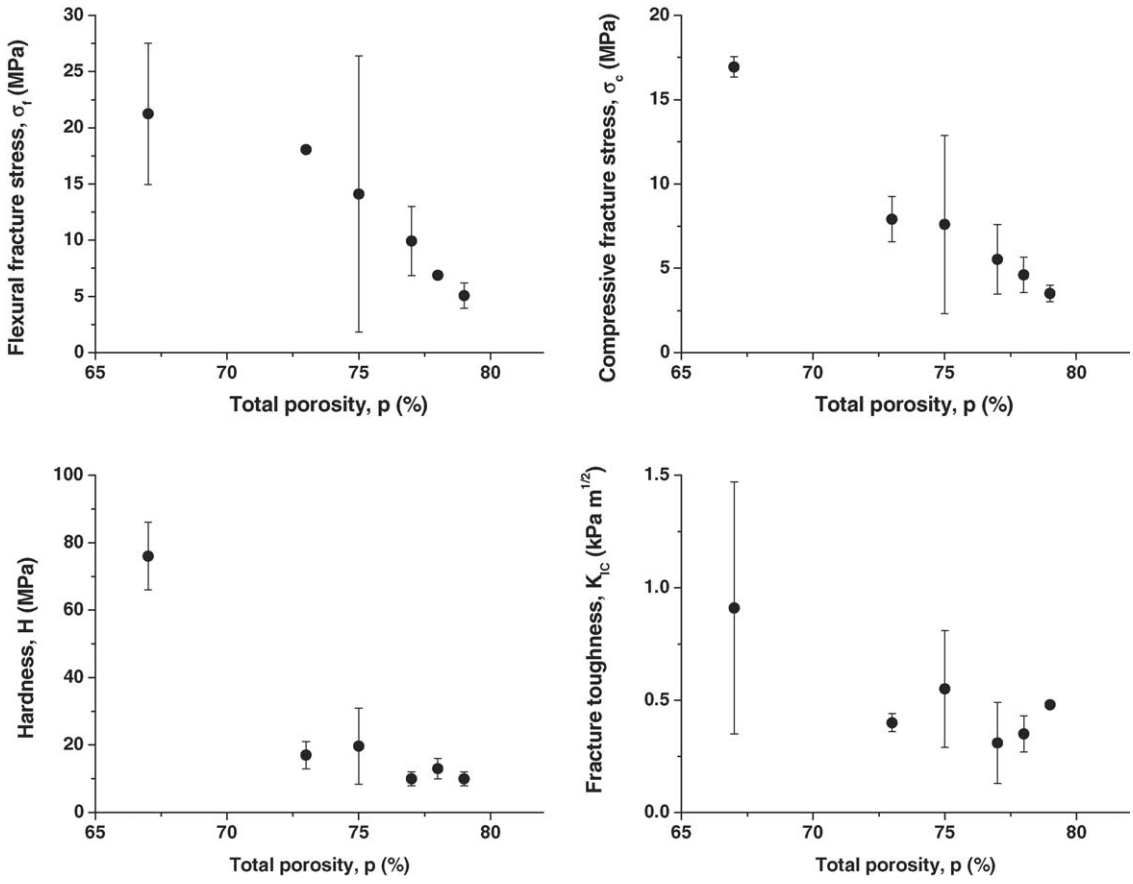

Fig. 3. Measured mechanical properties as a function of total porosity.

grains, for example spheres—by sintering. In their mathematical form, they present a major difference. Models describing the variation of mechanical properties with closed spherical porosity generally zero for a porosity of 100%. Indeed, starting from a dense body, it is always possible to place holes until nearly 100% porosity is reached, while keeping a continuous solid phase with a certain mechanical cohesion (even if some holes may interpenetrate). In this respect, it has been shown that the model proposed by Wagh et al.[17] was well adapted to describe the evolution of Young's modulus with porosity in ceramics. To obtain it, Wagh et al.[17] start from an initially dense body made of a stacking of identical bricks. Then, a random size reduction algorithm is applied to the bricks such as to create an increasing porosity. The material nevertheless retains its cohesion until 100% porosity, which writes, for the Young's modulus, E[17]:

$$E = E_0(1 - p)^m \tag{1}$$

E_0 is the Young's modulus of the fully dense material, and p the porosity volume fraction. The exponent m depends on the "tortuosity" of the porosity, but is usually close to 2.

At the opposite, equations describing the variation of mechanical properties with a porosity resulting from the incomplete densification by sintering of a pressed powder must zero for the porosity of the green body before sintering. Indeed, for this particular value of porosity, there is almost no mechanical cohesion since no chemical bond has yet developed between grains, but only weak electrostatic and/or friction forces. Then, as soon as the sintering process begins, necks start forming between grains, porosity decreases and mechanical properties take non-zero values. Several models of this category exist to describe the Young's modulus of sintered materials.[16,19,20] In particular, one of these models, proposed by Jernot et al.,[16] is based on an actual stereological description of the microstructure for different initial grain stacking geometries. It has proved very successful in describing the variation in Young's modulus with porosity for sintered metals, glasses and ceramics, despite its very simple mathematical expression:

$$E = E_0[N_C(1 - p) - (N_C - 1)(1 - p)^{2/3}] \tag{2}$$

N_C is the mean coordination number, i.e. the average number of neighbours of each grain in the microstructure. This expression tends towards zero for the porosity of the pressed powder before sintering, $p_0 = 1 - (1 - 1/N_c)^3$.

Besides, Wagh et al.[18] proposed an approach, based on energetic considerations during fracture, to set an equivalence between Young's modulus and toughness models for brittle materials. This procedure has been later corrected[23,32] to show that, if one can write the evolution of Young's modulus as a function of porosity as

$$E = E_0\, f(p) \tag{3}$$

then the variation of fracture toughness with porosity is given by

$$K_{IC} = K_{IC0}\, f(p) \tag{4}$$

where K_{IC0} is the toughness of the fully dense material.[24] It has also been suggested that such an equivalence would be valid only if the fracture micromechanisms remain the same over the whole range of investigated porosity.[23] The principle of this equivalence has been discussed and validated.[18,23,32] In particular, the approach is based on a calculation of the elastic energy stored in the specimen during loading (which involves the Young's modulus), and its restitution under the form of fracture energy. The specific fracture energy is then calculated as the ratio between the total rupture energy and the fracture surface area. This specific fracture energy is finally considered equal to the critical strain energy release rate, G_{IC}. It must be noted at this point that the latter is normally defined as the rate of energy transfer at the crack tip, and is not a global value over the whole fracture surface. However, the specific fracture energy is equal to the average value of G_{IC} over the whole fracture. And, in the case of brittle materials with no rising *R*-curve, G_{IC} is constant during crack extent and the specific fracture energy is therefore equal to G_{IC}.

To model the evolution of the mechanical properties of the present bioceramics, one could have chosen any of these models and tested it. However, it is worth reminding that a model is only to be used for what it has been made. In this respect, the models of Eqs. (1) and (2) could be adapted to the case of toughness, by following the approach explained above, but they would hold only for isolated closed pores or for a sintered stacking of grains, respectively, and only in the case of toughness. In the present case, on the one hand not only toughness is to be modelled but also fracture stress and hardness, and on the other hand the morphology of porosity does not correspond to either model. Indeed, two different kinds of porosities coexist in our bioceramics, with a very different morphology: isolated macropores and a continuous microporosity. Therefore, there is a need for a new modelling approach, based on an actual description of the microstructure.

4.2. Modelling approach

4.2.1. From Young's modulus to other mechanical properties

The first step of the modelling approach is to determine a procedure to obtain models for all investigated properties: toughness, fracture stress and hardness. For this, let us first assume that a model of the form $E = E_0\, f(p)$ exists for the Young's modulus, as in Eq. (3)—it will be derived in the next section. Of course, this model will not be used as it is, since no modulus measurement has been performed. Then, following the principle exposed in the previous section, the expression of Eq. (4) holds for toughness as long as the fracture micromechanisms remain the same over the whole range of porosity. This is the case for our materials, with a crack always going through macropores by fracturing the walls between pores, and by intergranular fracture at the grain scale (Fig. 2b–d). Therefore it is possible to accept Eq. (4).

The situation becomes more complex in the case of the fracture stress. Indeed, the latter is not usually an intrinsic material property, but is a technical datum resulting from the combination of both the fracture toughness and the size and geometry of the flaw on which fracture initiates, following:

$$\sigma_r = \frac{K_{IC}}{Y\sqrt{a_C}} \tag{5}$$

where σ_r is the fracture stress, a_C the critical flaw size and Y its associated geometrical factor. However, a quick calculation shows that for all the presently investigated materials, the critical flaw size is of the order of magnitude of the macropore size. This allows us to believe that the critical flaw is always one of the macropores. Because the latter are produced by the addition of a porogen of calibrated size, it becomes possible to assume that the critical flaw is almost constant in size and shape, and that, consequently, the associated geometrical factor, Y, is also the same for all our ceramics. So, if Y and a_C can be considered constant, and because Eq. (4) holds for toughness, it must be possible to write:

$$\sigma_r = \sigma_{r0}\, f(p) \tag{6}$$

where σ_{r0} is the strength of the perfectly dense ceramic. It is worth noting at this point that this approach cannot be applied to all brittle materials, but is specific to the present microstructures, where the critical flaw is not a natural processing defect but a microstructural element of nearly constant size and shape.

Modelling hardness is another complex issue, since an extended deformation occurs during the indentation process. Nevertheless, using simple considerations about the mechanical behaviour of ceramics under contact conditions, it is possible to apply our previous model. Indeed, during indentation, ceramics deform mainly by microcracking (Fig. 4a),[33–35] which is a fracture process. In this respect, our hardness tests can be better regarded as "crush tests", rather than classical indentation tests involving only a plastic deformation of the crystals. Therefore, as indentation is controlled by fracture, it must involve toughness and/or fracture stress, so that it should be possible to apply the same model for hardness as for toughness and strength, as:

$$H = H_0\, f(p) \tag{7}$$

where H_0 is the hardness of the dense body. However, because hardness involves an extended deformation, and a compaction of the porous body under the indenter[36,37] (Figs. 4a and 8), it is important to stress that this approach may give only very approximate results.

To sum up, if care is taken to assess all the hypotheses mentioned above (constancy of fracture mechanisms over the whole range of porosity, constancy in the critical flaw size and shape, indentation deformation governed by fracture mechanisms), the same function of porosity, $f(p)$, can be used to model any of the cited properties. Thus, if M is one of these mechanical properties and M_0 the property of the dense material, this writes:

$$M = M_0\, f(p) \tag{8}$$

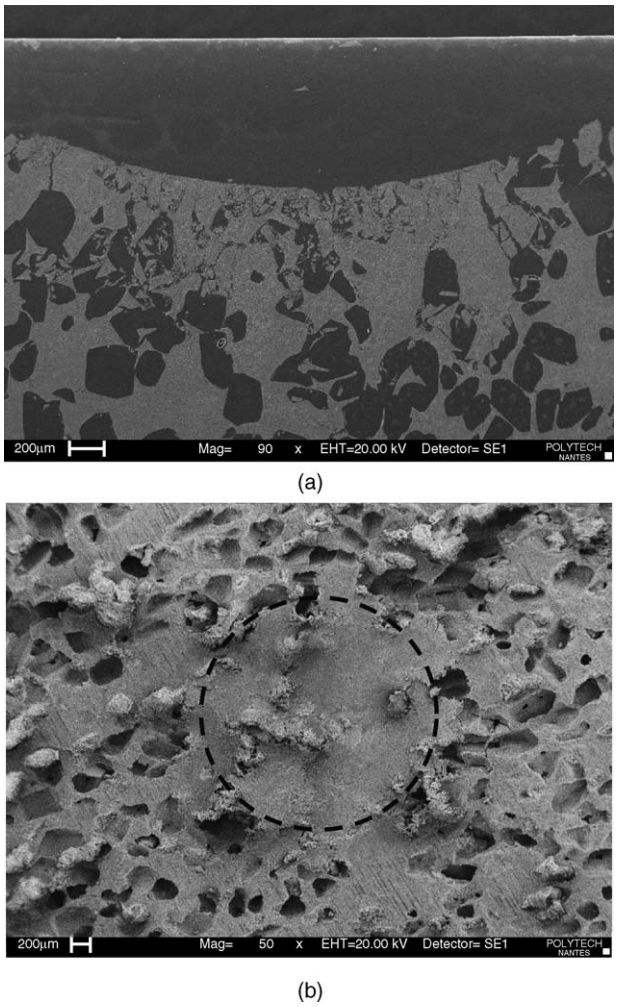

Fig. 4. (a) Polished cross-section of an indented surface: microcracking and compaction of the material under the indenter. (b) Top view of an indented surface: compaction of the material under the indenter.

M can be the Young's modulus, the toughness, the fracture stress or the hardness. The function of porosity, $f(p)$, is now to be calculated, which is done in the next section.

4.2.2. A new model for microporous and macroporous ceramics

To determine the function of porosity, $f(p)$, contrarily to what is generally made—for instance in Eqs. (1) and (2)—it is not appropriate here to express it as a function of the sole total porosity, p. Indeed, two types of porosities coexist in these ceramics, which are very different in their morphology (closed pores generated by the porogen and open porosity resulting from an incomplete sintering) and in their size (macropores of several hundreds of micrometer and micropore channels of the order of a micrometer). It is therefore not possible to use either of the two categories of models to describe the behaviour of our materials as a function of the total porosity. Because of this coexistence of the two main types of porosities, the following approach is a combination of both types of models. And, given that the two morphologies exist at two very different scales ("micro" and "macro"), they can be dissociated. Indeed, at the "macro" scale,

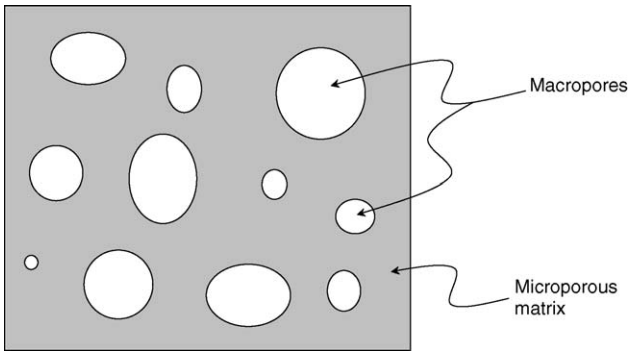

Fig. 5. Microstructural model: a microporous matrix containing isolated macropores.

these ceramics can be seen as a "continuous matrix" containing closed isolated macropores of several hundreds of micrometer, left by the elimination of the porogen (Fig. 2a and b). At the "micro" scale, the so-called "matrix" appears in fact as a microporous material with an open porosity resulting from the incomplete sintering of a pressed powder (Fig. 2d). These two statements are the base for the present microstructural model: a microporous matrix containing isolated macropores (Fig. 5).

Therefore, at the macropore scale, a closed porosity model can be used, like the one in Eq. (1). However, the value of porosity must be the sole macroporosity, p_{macro}, i.e. the fraction of the total volume occupied by macropores. For the Young's modulus, this writes:

$$E = E_{0\mathrm{m}}(1 - p_{\mathrm{macro}})^m \tag{9}$$

$E_{0\mathrm{m}}$ is thus the Young's modulus of the "continuous matrix", which is actually, at the "micro" scale, itself microporous. It is now necessary to define $E_{0\mathrm{m}}$ as a function of microporosity, p_{micro}, the latter being the fraction of the "matrix" volume occupied by micropores. Because this matrix is the result of the incomplete sintering of a pressed powder, a model of the second category, like the one in Eq. (2), can be used. This gives:

$$E_{0\mathrm{m}} = E_0[N_{\mathrm{C}}(1 - p_{\mathrm{micro}}) - (N_{\mathrm{C}} - 1)(1 - p_{\mathrm{micro}})^{2/3}] \tag{10}$$

By combining Eqs. (9) and (10), a model is obtained to describe the evolution of the Young's modulus with the two types of porosity:

$$E = E_0[N_{\mathrm{C}}(1 - p_{\mathrm{micro}}) - (N_{\mathrm{C}} - 1)(1 - p_{\mathrm{micro}})^{2/3}] \times (1 - p_{\mathrm{macro}})^m \tag{11}$$

Finally, using the assumptions of Section 4.2.1, three additional models are calculated for fracture toughness, fracture stress and hardness:

$$K_{\mathrm{IC}} = K_{\mathrm{IC0}}[N_{\mathrm{C}}(1 - p_{\mathrm{micro}}) - (N_{\mathrm{C}} - 1)(1 - p_{\mathrm{micro}})^{2/3}] \times (1 - p_{\mathrm{macro}})^m \tag{12}$$

$$\sigma_{\mathrm{r}} = \sigma_{\mathrm{r0}}[N_{\mathrm{C}}(1 - p_{\mathrm{micro}}) - (N_{\mathrm{C}} - 1)(1 - p_{\mathrm{micro}})^{2/3}] \times (1 - p_{\mathrm{macro}})^m \tag{13}$$

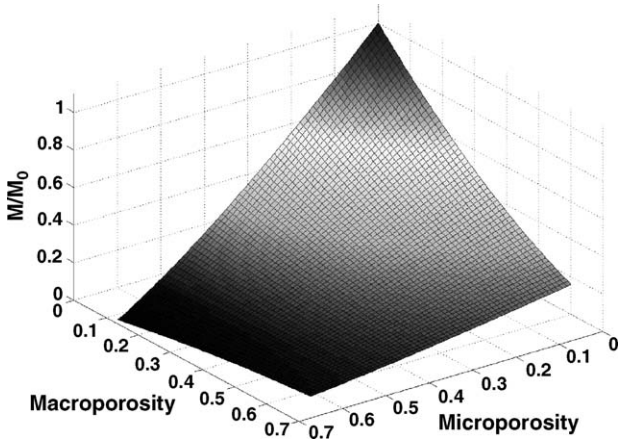

Fig. 6. Possible 3D representation of the theoretical model: normalised mechanical property, M/M_0, as a function of both microporosity and macroporosity.

$$H = H_0[N_C(1 - p_{micro}) - (N_C - 1)(1 - p_{micro})^{2/3}] \times (1 - p_{macro})^m \quad (14)$$

Each model is a function of two variables, p_{micro} and p_{macro}, and makes use of three adjustable parameters: N_C, m, and the property of the material at zero porosity, M_0. To represent completely such models, one can plot either a three-dimensional graph or, in two dimensions, plot "iso-macroporosities" as a function of microporosity, or "iso-microporosities" as a function of macroporosity. Examples of such theoretical models are represented in Figs. 6 and 7, with arbitrarily chosen values of $m = 2$ and $N_C = 5$.

4.3. Results and discussion

It is obvious that such models are rather difficult to adjust to experimental measurements, since they imply three parameters. Moreover, in the present case, macroporosity is similar for all ceramics—from 0.44 to 0.485—because it results mainly from the initial amount of porogen, which is the same for all specimens. However, the present results constitute a preliminary assessment of the validity of the proposed model, and other measurement, with a variation in macroporosity, will be necessary in the future. It is therefore almost impossible to determine the exponent m by adjusting the models to data. For this reason, we shall take $m = 2$, which is a rather common value for ceramic materials.[17,18] Consequently, the only "true" variable for our bioceramics is microporosity, p_{micro}, and there are only two adjustable parameters for each model, N_C and M_0. However, given that the same materials have been used to measure all properties, the mean coordination number, N_C, must be common to all models.

To sum up, there is a total of five adjustable parameters (N_C, K_{IC0}, σ_{c0}, σ_{f0} and H_0) for four sets of experimental data (toughness K_{IC}, compressive strength σ_c, flexural strength σ_f and hardness H). Optimal parameters, determined by a simultaneous adjustment of the models to experimental data, are the following:

$$N_C = 3, \quad \sigma_{f0} = 220\,\text{MPa}, \quad \sigma_{c0} = 135\,\text{MPa}$$
$$m = 2, \quad H_0 = 340\,\text{MPa}, \quad K_{IC0} = 8.6\,\text{MPa m}^{1/2}$$

For plotting purposes, as macroporosity is comprised between 44% and 48.5%, two extreme models have been computed for each mechanical property, one with $p_{macro} = 0.44$, the other with $p_{macro} = 0.485$. These two extreme models are then plotted for each property as a function of microporosity, and compared to measured values (Fig. 8).

Overall results are rather good, if the high statistical dispersion of measurements is taken into account. One single point seems significantly far from the model curves, in the case of hardness. In fact, hardness measurements present a major difference compared to the other ones in that they have been performed under different loads for the various materials. Indeed, depending on hardness, a more or less important load had to be applied to obtain a good penetration of the indenter and an easily measurable indent. As the fracture mechanisms involved during indentation may be sensitive to load, it is probable that this peculiar point actually reflects a change in fracture and deformation micromechanisms with load (as this ceramic is the hardest of all, a significantly higher load had to be applied).

All other results are globally satisfying. In fact, another aspect has not been mentioned so far that can help to understand the observed statistical dispersion: the uncertainty on porosity measurements. Indeed, macroporosity is measured by

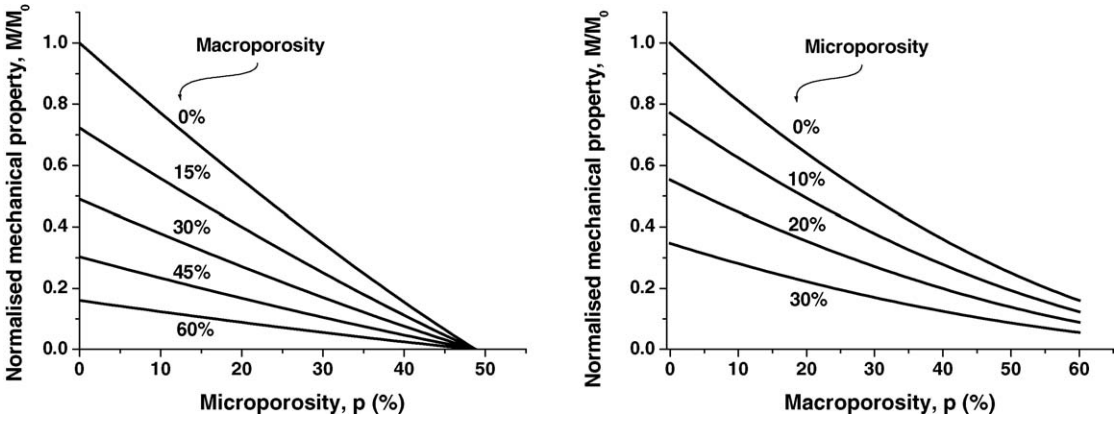

Fig. 7. Possible 2D representations of the theoretical model: "iso-macroporosities" as a function of microporosity, and "iso-microporosities" as a function of macroporosity.

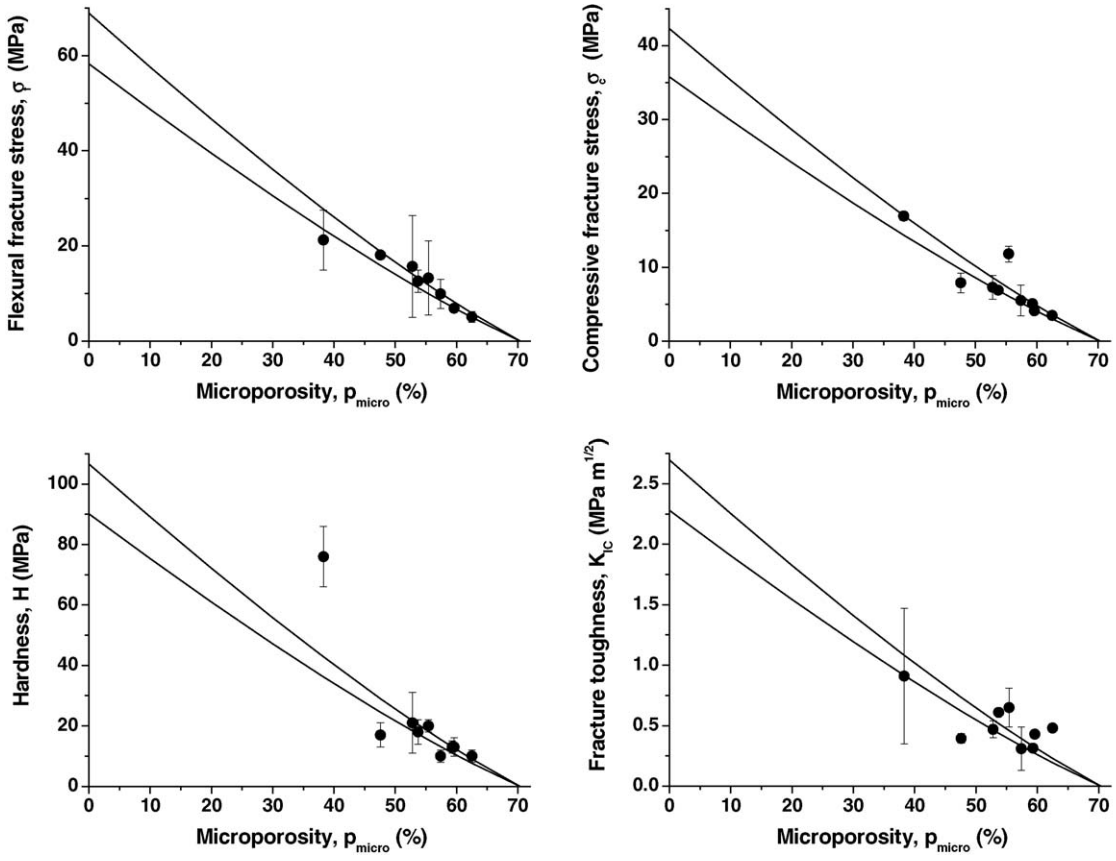

Fig. 8. Comparisons of the models with the measured mechanical properties.

quantitative image analysis on polished cross-sections, which can yield absolute errors of a few %. Total porosity is determined by the weight method on parallelepipedic bars, which can also give a few % of absolute error. Finally, microporosity is deduced from these two values. As, in the investigated domain, the variation of mechanical properties with microporosity is extremely steep, important relative errors can be the consequence of small absolute errors on porosity values. For example, with $p_{\text{macro}} = 45\%$, for $p_{\text{micro}} = 62\%$, $M/M_0 = 0.027$; and for $p_{\text{micro}} = 60\%$, $M/M_0 = 0.035$. This represents a relative error of 30% on M/M_0, whereas the difference in microporosities is only two points.

Besides, a mean coordination number of three is obtained. This could be considered surprising for a stacking of grains resulting from the sintering of a pressed powder, since values between five and seven are usually observed for sintered materials.[16,23,24] It is nevertheless consistent with the very high microporosities measured on the one hand (up to more than 62%), and with the microscopic and fractographic observations on the other hand (Fig. 2d).

Finally, the adjustment of parameters indicates that, contrarily to what could be originally thought, the measured mechanical properties are not abnormally low. Indeed, fracture stresses and hardnesses from 135 to 340 MPa are obtained for the fully dense material, as well as a toughness of 8.6 MPa $m^{1/2}$. These "virtual" values for the dense body may seem very high for such materials, but are not surprising when considering already published measurements on less porous and properly sintered apatite ceramics. For instance, Le Huec et al.[25] have measured a fracture stress of 348 MPa for HA ceramics containing 22.5% porosity, which could even be extrapolated to more than 1200 MPa for the virtual bulk. In other words, it has already been reported that calcium phosphate bioceramics are intrinsically strong materials, and the fact that our extrapolated values compare with those of structural ceramics, like alumina, zirconia or silicon nitride, is not abnormal. However, it is here important to note that such "virtual" values may not be reachable for actual dense materials, as the fracture micro mechanisms may change when porosity is reduced. Anyway, the presently developed models show that our ceramics are properly processed, but that their low mechanical properties only lie in their very high porosity. In this respect, the role of modelling is interesting since, even if it cannot be used as a proper predictive tool, it is a way to explain and understand experimental observations.

5. Conclusions and perspectives

Macroporous biphasic (HA/TCP) calcium phosphate bioceramics, for application as bone substitutes, have been synthesized, pressed and pressureless sintered under air. Their mechanical properties, investigated by conventional techniques and by indentation, are very low and subject to a high statistical dispersion. New models, based on a geometrical description of the microstructure as a microporous "matrix" containing isolated

closed macropores, could explain this peculiar behaviour and the dispersion of measured values. However, such models will be completely validated only if additional measurements are provided, on extended ranges of macroporosity and microporosity (from a nearly dense ceramic, without the addition of a porogen, to the presently investigated highly porous materials). Experimental work is currently carried out to obtain additional mechanical data, in an attempt to validate completely the modelling approach. Then, as it has already been observed and modelled on other sintered materials,[24] changes in fracture micromechanisms may occur, which would raise a need for more complex models. For instance, if no porogen is added, the critical flaw could not be a macropore anymore.

Finally, for future applications, it seems that it would be necessary to decrease the amount of porosity, in particular the microporosity as, in the investigated and modelled range, it exhibits a strong influence on mechanical properties. It will be therefore interesting to study the experimental influence of processing parameters—porogen content, compaction pressure, sintering temperature and time—on microstructure and on both mechanical and biological properties. From all these aspects, it is clear that the amount, size and morphology of porosity must be precisely balanced and controlled in order to optimise the overall performance of these bioceramics.

Acknowledgments

F. Tancret would like to express his gratitude to his former Ph.D. supervisor, late Dr. Frédéric Osterstock, for his indirect contribution to this work through passionate discussions on mechanical properties of porous materials, but above all for friendship over 10 years.

References

1. Nery, E. B., Lynch, K. L., Hirthe, W. M. and Mueller, K. H., Bioceramic implants in surgically produced infrabony defects. *J. Periodontol.*, 1975, **46**(6), 328–347.
2. Jarcho, M., Bolen, H., Thomas, M. B., Bobick, J., Kay, J. K. and Doremus, R. H., Hydroxylapatite synthesis and characterization in dense polycristalline form. *J. Mater. Sci.*, 1976, **11**(11), 2027–2035.
3. Jarcho, M., Calcium phosphate ceramics as hard tissue prosthetics. *Clin. Orthop.*, 1981, **157**, 259–278.
4. Ransford, A. O., Morley, T., Edgar, M. A., Webb, P., Passuti, N., Chopin, D. *et al.*, Synthetic porous ceramic compared with autograft in scoliosis surgery. *J. Bone Joint Surg. (B)*, 1998, **80**(1), 13–18.
5. Passuti, N., Daculsi, G., Rogez, J. M., Martin, S. and Bainvel, J. V., Macroporous calcium phosphate ceramic performance in human spine fusion. *Clin. Orthop.*, 1989, **46**(248), 169–176.
6. Delecrin, J., Takahashi, S., Gouin, F. and Passuti, N., A synthetic porous ceramic as a bone graft substitute in the surgical management of scoliosis: a prospective, randomized study. *Spine*, 2000, **25**(5), 563–569.
7. Daculsi, G., Bouler, J. M. and LeGeros, R. Z., Adaptive crystal formation in normal and pathological calcifications in synthetic calcium phosphate and related biomaterials. *Int. Rev. Cytol.*, 1997, **172**, 129–191.
8. Yamada, S., Heymann, D., Bouler, J. M. and Daculsi, G., Osteoclastic resorption of calcium phosphate ceramics with different hydroxyapatite/β-tricalcium phosphate ratios. *Biomaterials*, 1997, **18**(15), 1037–1041.
9. Daculsi, G., Laboux, O., Malard, O. and Weiss, P., Current state of the art of biphasic calcium phosphate bioceramics. *J. Mater. Sci.: Mater. Med.*, 2003, **14**(3), 195–200.
10. LeGeros, R. Z., Daculsi, G., Orly, I., Gregoire, M., Heughebaert, M., Gineste, M. *et al.*, Formation of carbonated apatite on calcium phosphate materials: dissolution/precipitation processes. In *Bone Bonding*, ed. Ducheyne, Kokubo and van Blitterswijk. Reed Healthcare Communications, 1992, pp. 201–212.
11. Malard, O., Bouler, J. M., Guicheux, J., Heymann, D., Pilet, P., Coquard, C. *et al.*, Influence of biphasic calcium phosphate granulometry on bone ingrowth, ceramic resorption, and inflammatory reactions. Preliminary in vitro and in vivo study. *J. Biomed. Mater. Res.*, 1999, **46**(1), 103–111.
12. Gauthier, O., Bouler, J. M., Aguado, E., Pilet, P. and Daculsi, G., Macroporous biphasic calcium phosphate ceramics: influence of macropore diameter and macroporosity percentage on bone ingrowth. *Biomaterials*, 1998, **19**(1–3), 133–139.
13. Ellinger, R. F., Nery, E. B. and Lynch, K. L., Histological assessment of periodontal osseous defects following implantation of hydroxyapatite and biphasic calcium phosphate ceramics: a case report. *Int. J. Periodont. Restor. Dent.*, 1986, **6**(3), 22–33.
14. Daculsi, G., Weiss, P., Bouler, J. M., Gauthier, O., Millot, F. and Aguado, E., Biphasic calcium phosphate/hydrosoluble polymer composites: a new concept for bone and dental substitution biomaterials. *Bone*, 1999, **25**(2, Suppl. 1), 59S–61S.
15. Bouler, J. M., Trecant, M., Delecrin, J., Royer, J., Passuti, N. and Daculsi, G., Macroporous biphasic calcium phosphate ceramics: influence of five synthesis parameters on compressive strength. *J. Biomed. Mater. Res.*, 1996, **32**(4), 603–609.
16. Jernot, J. P., Coster, M. and Chermant, J. L., Model to describe the elastic modulus of sintered materials. *Physica Status Solidi (a)*, 1982, **72**(1), 325–332.
17. Wagh, A. S., Poeppel, R. B. and Singh, J. P., Open pore description of mechanical properties of ceramics. *J. Mater. Sci.*, 1991, **26**(14), 3862–3868.
18. Wagh, A. S., Singh, J. P. and Poeppel, R. B., Dependence of ceramic fracture properties on porosity. *J. Mater. Sci.*, 1993, **28**(13), 3589–3593.
19. Arató, P., Besenyei, E., Kele, A. and Wéber, F., Mechanical properties in the initial stage of sintering. *J. Mater. Sci.*, 1995, **30**(7), 1863–1871.
20. Rice, R. W., Comparison of stress concentration versus minimum solid area based mechanical property-porosity relations. *J. Mater. Sci.*, 1993, **28**(8), 2187–2190.
21. Rice, R. W., Evaluation and extension of physical property-porosity models based on minimum solid area. *J. Mater. Sci.*, 1996, **31**(1), 102–118.
22. Boccaccini, A. R., Fabrication, microstructural characterisation and mechanical properties of glass compacts containing controlled porosity of spheroidal shape. *J. Porous Mater.*, 1999, **6**(4), 369–379.
23. Tancret, F., Desgardin, G. and Osterstock, F., Influence of porosity on the mechanical properties of cold isostatically pressed and sintered $YBa_2Cu_3O_{7-x}$ superconductors. *Philos. Mag. A*, 1997, **75**(2), 505–523.
24. Tancret, F. and Osterstock, F., Modelling the toughness of porous sintered glass beads with various fracture mechanisms. *Philos. Mag.*, 2003, **83**(1), 137–150.
25. Le Huec, J. C., Schaeverbeke, T., Clement, D., Faber, J. and Le Rebeller, A., Influence of porosity on the mechanical resistance of hydroxyapatite ceramics under compressive stress. *Biomaterials*, 1995, **16**(2), 113–118.
26. Bouler, J. M., LeGeros, R. Z. and Daculsi, G., Biphasic calcium phosphates: influence of three synthesis parameters on the HA/β-TCP ratio. *J. Biomed. Mater. Res.*, 2000, **51**(4), 680–684.
27. Friel, J. J., *Practical Guide to Image Analysis*. ASM International, 1992.
28. Jouin, J. M., *Propagation à température ambiante de défauts dans des matériaux céramiques*. Ph.D. thesis, University of Caen, France, 1986.
29. Toth, J. M., Hirthe, W. M., Hubbard, W. G., Brantley, W. A. and Lynch, K. L., Determination of the ratio of HA/TCP mixtures by X-ray diffraction. *J. Appl. Biomater.*, 1991, **2**(1), 37–40.
30. Ishikawa, K., Ducheyne, P. and Radine, S., Determination of the Ca/P ratio in calcium-deficient hydroxyapatite using X-ray diffraction analysis. *J. Mater. Sci.: Mater. Med.*, 1993, **4**(2), 165–168.
31. Tancret, F., Comment on 'Mechanical properties in the initial stage of sintering'. *J. Mater. Sci. Lett.*, 2000, **19**(17), 1557–1558.

32. Arató, P., Comment on 'dependence of ceramics fracture properties on porosity'. *J. Mater. Sci. Lett.*, 1996, **15**(1), 32–33.
33. Suganuma, M., Scanning acoustic microscopy of indentation damage in Y_2O_3-stabilized tetragonal zirconia. *J. Am. Ceram. Soc.*, 1995, **78**(11), 2889–2896.
34. Pinot, L., *Apparition et développement de l'endommagement par contact pointu sur des cermets WC-Co*. Masters thesis, University of Caen, France, 1996.
35. Legendre, B., *Le transfert thermique pendant la trempe; apport du choc thermique des céramiques*. Ph.D. thesis, University of Caen, France, 1997.
36. Tancret, F. and Osterstock, F., Indentation behaviour of porous materials: application to the Vickers indentation cracking of ceramics. *Philos. Mag.*, 2003, **83**(1), 125–136.
37. Tancret, F. and Osterstock, F., Influence of porosity on the hydrostatic constraint factor for evaluating toughness from Vickers indentation cracks in brittle materials. *Philos. Mag. Lett.*, 2004, **84**(1), 1–6.